doi:10.1006/jmbi.2000.4095 available online at http://www.idealibrary.com on IDEAL® J. Mol. Biol. (2000) 302, 927–940

JMB

II. Structure and Specificity of the Interaction between the FHA2 Domain of Rad53 and Phosphotyrosyl Peptides†

Peng Wang, In-Ja L. Byeon*, Hua Liao, Kirk D. Beebe Suganya Yongkiettrakul, Dehua Pei* and Ming-Daw Tsai*

Departments of Chemistry and Biochemistry, The Ohio State Biochemistry Program, and Campus Chemical Instrument Center, The Ohio State University, Columbus OH 43210, USA

**Corresponding authors*

The forkhead-associated (FHA) domain is a protein module found in many proteins involved in cell signaling in response to DNA damage. It has been suggested to bind to pThr sites of its target protein. Recently we have determined the first structure of an FHA domain, FHA2 from the yeast protein Rad53, and demonstrated that FHA2 binds to a pTyr-containing peptide ^{826}EDI(pY)YLD^{832} from Rad9, with a moderate affinity (K_d ca. 100 μM). We now report the solution structure of the complex of FHA2 bound with this pTyr peptide. The structure shows that the phosphate group of pTyr interacts directly with three arginine residues (605, 617, and 620), and that the leucine residue at the +2 position from the pTyr interacts with a hydrophobic surface on FHA2. The sequence specificity of FHA2 was determined by screening a combinatorial pTyr library. The results clearly show that FHA2 recognizes specific sequences C-terminal to pTyr with the following consensus: XX(pY)$N_1N_2N_3$, where N_1 = Leu, Met, Phe, or Ile, N_2 = Tyr, Phe, Leu, or Met, and N_3 = Phe, Leu, or Met. Two of the selected peptides, GF(pY)LYFIR and DV(pY)FYMIR, bind FHA2 with K_d values of 1.1 and 5.0 μM, respectively. The results, along with other recent reports, demonstrate that the FHA domain is a new class of phosphoprotein-binding domain, capable of binding both pTyr and pThr sequences.

Keywords: FHA domain; Rad53; phosphotyrsine; phosphopeptide

Introduction

Protein-protein interaction is one of the essential mechanisms used in cellular signaling processes. Interactions between two proteins are often mediated by small modular domains, which are autonomously folded and recognize short stretches of amino acid residues in their partner proteins. A number of such modules, including SH2, SH3, PTB, and 14-3-3 domains, have been identified in signaling proteins of organisms from yeast to human (Pawson & Scott, 1997). Recently, a new module, the forkhead-associated (FHA) domain, has been identified by sequence analyses (Hofmann & Bucher, 1995). It was first identified within a subset of forkhead transcriptional factors, located outside of the conserved DNA-binding forkhead domain. It was subsequently found in more than 20 other proteins, mostly nuclear protein kinases and transcriptional factors. New FHA-containing proteins of diverse functions continue to be identified. More recent additions include HuCdsl (or Chk2) from humans (Brown *et al.*, 1999; Matsuoka *et al.*, 1998) and Dmnk from *Drosophila melanogaster* (Oishi *et al.*, 1998). Both proteins participate in the cellular response to DNA damage. Recently, an FHA domain was identified

†Paper I in this series is Liao *et al*. (1999).

Abbreviations used: B, β-alanine; EDTA, ethylenediamine tetraacetic acid; FHA, forkhead-associated domain; FRET, fluorescence energy transfer; GST, glutathione S-transferase; HBTU, 2-(1*H*-benzotriazole-1-yl)-1,1,3,3-tetramethyluronium hexafluorophosphate; HOBT, 1-hydroxybenzotriazole; HSQC, heteronuclear single-quantum coherence; MALDI, matrix-assisted laser desorption ionization; MS, mass spectroscopy; Nle, norleucine; NOE, nuclear Overhauser enhancement; NOESY, nuclear Overhauser enhancement correlated spectroscopy; PTB domain, phosphoprotein-binding domain.

E-mail addresses of the corresponding authors: Byeon.2@osu.edu, Pei.3@osu.edu, Tsai.7@osu.edu

0022-2836/00/040927–14 $35.00/0

in the N terminus of nuclear RNA-binding protein NIPP1 (Boudrez *et al*., 2000). It has been suggested that the FHA domain is involved in the regulation of pre-mRNA splicing.

The FHA domain was initially defined as having approximately 55-75 amino acid residues with three conserved regions. However, our NMR structure of the FHA2 domain of Rad53 (residues 573-730) indicates that the FHA2 domain of Rad53 requires approximately 160 amino acid residues to fold into a stable three-dimensional (3D) structure (Liao *et al*., 1999), which is considerably larger than previously predicted on the basis of sequence homology (55-75 amino acid residues). Sun *et al*. (1998) also reported that deletion of 52 amino acid residues from either end of a functional fragment of Rad53 (residues 549-730) abolished its interaction with Rad9. Hammet *et al*. (2000) reported that the Dun1p FHA domain also contained 130-140 amino acid residues. Furthermore, in a subset of FHA domains, sequence homology extends beyond the originally defined region in both directions by 25 to 30 residues (Boudrez *et al*., 2000).

FHA has been proposed to be a new phosphoprotein binding domain (Hofmann & Bucher, 1995), which is supported by extensive experimental evidence. However, it remains to be established whether the FHA domain recognizes pSer/pThr or pTyr peptides. The FHA domain of kinase-associated protein phosphatase (KAPP) from *Arabidopsis thaliana* binds to a phosphorylated receptor-like protein kinase RLK5 (Li *et al*., 1999). Likewise, the FHA domain of NIPP1 interacts with CDC5L in a phosphorylation-dependent manner (Boudrez *et al*., 2000). Rad53, a yeast checkpoint protein involved in the DNA damage response (Allen *et al*., 1994; Zheng *et al*., 1993), contains two FHA domains and binds to phosphorylated Rad9 (Sun *et al*., 1998; Durocher *et al*., 1999). In most of these cases, the reported evidence seems to suggest FHA as a pSer/pThr binding domain. For instance, the N-terminal FHA domain of Rad53 (FHA1) binds to a pThr peptide derived from p53 ($K_d \sim 2$ μM), and this pThr peptide is capable of disrupting the association between FHA1 and phosphorylated Rad9 (Durocher *et al*., 1999). On the other hand, we have previously shown that a pTyr peptide derived from Rad9, ^{826}EDI(pY)YLD^{832}, binds to the FHA2 domain of Rad53 with a moderate affinity ($K_d \sim 100$ μM; Liao *et al*., 1999). These results taken together led us to propose that FHA domains may have dual specificity, or different FHA domains may recognize different phosphoamino acids.

In our previous paper, we described our determination of the solution structure of the FHA2 domain of Rad53 (Liao *et al*., 1999). Here, we report the refined FHA2 domain structure and the FHA2-pTyr peptide (^{826}EDI(pY)YLD^{832} from Rad9) complex structure. In addition, by screening a combinatorial library of pTyr peptides, we have identified specific pTyr peptides which bind to FHA2 with low μM K_d values.

Results and Discussion

Refined solution structure of free FHA2

The solution structure of the FHA2 domain of yeast Rad53 was refined by adding 410 NOE restraints and 188 TALOS-derived backbone torsion angle restraints and by revising a few misassigned NOEs. The addition and revision of NOE restraints were based on iterative analyses between the structure and the NOE restraints. We have also included the TALOS restraints in structure calculations because they were in excellent agreement with secondary structures predicted from NMR data. Although they show basically the same topology, a β-sandwich and a C-terminal α-helix, the refined structures have much improved quality (Table 1) relative to the previously published structures (Liao *et al*., 1999). They satisfy the experimental distance restraints better (r.m.s.d. decreased from 0.042 Å to 0.033 Å), display smaller deviations from idealized covalent geometry (0.004 Å to 0.003 Å for bonds, 0.69° to 0.47° for angles and 0.52° to 0.4° for impropers), exhibit a better Ramachandran plot (54% to 83% for most favored regions), and have good non-bonded contacts ($E_{L\text{-}J} = -290$ kcal/mol). Furthermore, the structures converge much better (Figure 1(a) and Table 1): excluding the disordered loops, 632-642 and 706-713, and the N and C-terminal residues, the r.m.s.d. values are 0.37(±0.05) Å (compared to 0.51(±0.09) Å) and 0.83(±0.05) Å) (compared to 0.97(±0.09) Å) for backbone and all heavy atoms, respectively. The following points are worth mentioning regarding the structural improvement observed from the refined structures. First, the C-terminal helix becomes longer, consisting of residues 721-729 (Figure 1(b)). The problem of having an abnormal kink at the C-terminal helix in the previous structure (Liao *et al*., 1999) has now been resolved. Second, the two central β-strands, β9 and β10, of the lower β-sheet are extended to consist of residues 676-683 and 688-696, respectively (Figure 1(b)). Note that the β9 strand has a bulge at Val680. Finally, one more β-strand, β3′ (residues 611-613), is added to the top β-sheet. In contrast to the other 11 strands that are in antiparallel β-sheets, this strand forms a parallel β-sheet with its partner strand, β3.

Solution structure of the FHA2-pTyr peptide complex

We have previously reported that a pTyr-containing peptide, ^{826}EDI(pY)YLD^{832} derived from Rad9, binds FHA2 with a K_d value of ~100 μM. The superimposed ^{15}N-HSQC spectra of the free and the peptide-complexed FHA2 show that several backbone NH groups undergo significant shifts upon peptide binding (Figure 2). The side-chain N$^{\varepsilon}$H groups of Arg605, Arg617, and Arg620 are also shifted. In contrast, the peptide spectrum (not shown) exhibits only small shifts

Table 1. Structural statistics for the refined FHA2 structures

	⟨SA⟩	($\overline{SA}$)r
r.m.s.d. from experimental distance restraints (Å)[a]		
All (3061)	0.033 ± 0.001	0.033
Sequential ($\|i-j\|=1$) (615)	0.040 ± 0.003	0.041
Medium ($1<\|i-j\|<5$) (306)	0.044 ± 0.002	0.045
Long range ($\|i-j\|\geqslant 5$) (1163)	0.028 ± 0.001	0.030
Intraresidue (897)	0.029 ± 0.001	0.028
Hydrogen bonds (80)	0.017 ± 0.002	0.018
r.m.s.d. from backbone torsion angle restraints (°) (188)[b]	1.959 ± 0.045	1.972
r.m.s.d. from idealized covalent geometry:		
Bonds (Å)	0.003 ± 0.000	0.003
Angles (°)	0.465 ± 0.010	0.475
Impropers (°)	0.395 ± 0.016	0.384
Final energy:		
E_{L-J} (kcal/mol)[c]	−289 ± 67	−284
PROCHECK (Ramachandran plot)[d]		
Most favored regions (%)	82.6 ± 1.6	82.0
Additionally allowed region (%)	15.4 ± 1.5	16.4
Generously allowed region (%)	0.1 ± 0.3	0.0
Disallowed region (%)	1.7 ± 0.3	1.6
Atomic r.m.s.d. between ⟨SA⟩ and $\overline{SA}$ (Å):	Backbone	All heavy atoms
Residues 575-631, 643-705, and 714-729	0.37 ± 0.05	0.83 ± 0.05

⟨SA⟩ are the final 19 simulated annealing structures; $\overline{SA}$ is the mean structure obtained by averaging the coordinates of the individual SA structures best fit to each other (excluding the flexible N-terminal (573-574), loop (632-642 and 706-713), and C-terminal (730) residues); and ($\overline{SA}$)r is the restrained minimized mean structure obtained by restrained minimization of the mean structure $\overline{SA}$. The number of restraints is given in parentheses.

[a] None of the ⟨SA⟩ structures exhibited distance violations greater than 0.5 Å.

[b] The torsion angle restraints were derived by using TALOS (Cornilescu *et al.*, 1999).

[c] E_{L-J} is the Lennard-Jones van der Waals energy calculated with the X-PLOR PARMALLH6 protein parameters (Brünger, 1992) and is not included in the target function for simulated annealing or restrained minimization.

[d] The flexible loop (632-642 and 706-713) residues are excluded from the statistics.

(0.05-0.07 ppm) upon binding to FHA2, and the shifts are observed only for pTyr and the residues at the −1, +1, and +2 positions. The small magnitude of shifts in the peptide resonances could be the result of several factors: moderate binding affinity, the peptide is in excess of the protein and is in fast exchange at the NMR time scale, and the extended conformation of bound peptide.

The solution structure of the FHA2-pTyr peptide complex was subsequently determined. Intermolecular NOE distance restraints were obtained mostly from the 3D ^{13}C-edited (f_2), ^{13}C/^{15}N-filtered (f_3) NOESY experiment (Figure 3). The NOEs mainly came from the pTyr and the Leu at the +2 position of the peptide. A total of 18 intermolecular distance restraints were deduced from such NOE analyses. On the basis of the analysis of the HSQC spectra described in the previous paragraph, three additional distance restraints (4.3(±0.3) Å for the C^{ζ} of Arg605, Arg617, and Arg620 to the P atom of pTyr) were included in the calculation of the complex structure. The complex structures generated without using the artificial distance restraints clearly showed that the Arg side-chain amino groups are close to the pTyr phosphate group. The 19 superimposed complex structures are shown in Figure 4(a) and a summary of structural statistics is provided in Table 2. The complex structures satisfy the experimental restraints very well, and show good covalent geometry, non-bonded energy and Ramachandran plot (Table 2). The structures of the FHA2 domain in the complex are very well converged, with r.m.s.d. values of 0.36(±0.05) Å and 0.80(±0.05) Å for the backbone and all heavy atoms, respectively. However, the peptide structures are less well converged: the r.m.s.d. values for the structured region of the peptide (the residues at the 0 to +2 positions) are 1.32(±0.40) Å and 2.18(±0.56) Å for the backbone and all heavy atoms, respectively (Table 2 and Figure 4(a)).

Structural comparison of FHA2 in free and complexed forms

Figure 4(b) shows the superimposed backbone structures of the free and complexed FHA2 along with three arginine side-chains at the binding site. The FHA2 domain undergoes little backbone structural change upon peptide binding, as indicated by small r.m.s.d. values between the free and bound forms (Table 2). This is a reflection of the fact that the FHA2-peptide complex, excluding the 21 intermolecular NOES, gave largely the same set of NOEs as the free protein (except for 26 out of >3000 NOEs). The most interesting and clear NOE difference is that relatively strong NOEs were observed between the β protons of Ser606 and the δ protons of Arg620 in the complex but not in the free protein. Note that Arg620 undergoes the largest spectral shift upon binding (Figure 2). In fact, the side-chain of Arg620 moves by as much as 2.1 Å upon peptide binding (Figure 4(b)). The r.m.s.d. value for the Arg620 side-chain atoms is decreased from 1.92 Å to 0.47 Å, indicating that

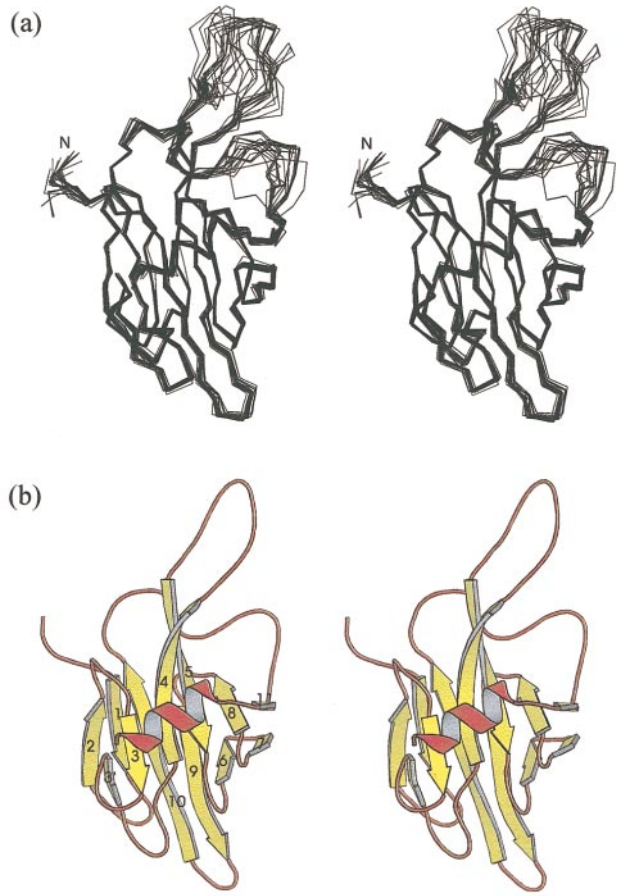

Figure 1. (a) Stereoview showing the superposition of the backbone C^{α} atoms of the 19 lowest-energy structures of the refined FHA2 domain. (b) Stereoview of the schematic ribbon diagram of the restrained minimized mean structure. Insight II (Molecular Simulations Inc.) and MOLSCRIPT (Kraulis, 1991) were used for (a) and (b), respectively.

the flexible side-chain becomes less mobile upon binding. These results taken together suggest that binding of the peptide to FHA occurs by repositioning a few critical side-chains without causing backbone perturbation. Note that the Lennard-Jones energy of the FHA2-peptide complex is about 40-60 kcal/mol lower than that of the free FHA2.

Detailed interactions between FHA2 and the phosphotyrosine peptide

Figure 5 shows the interactions between FHA2 and the peptide. The pTyr phosphate group of the peptide interacts with the guanidino groups of Arg605, Arg617, and Arg620, which reside in the loops connecting strands β3 and β3′, and β3′ and β4. These guanidino groups, which are spatially close in the free form, come even closer upon peptide binding (Figure 4(b)). Ser619 is also in close contact with the phosphate group. These interactions with the phosphate group presumably constitute a major portion of the overall binding energy, because unphosphorylated peptide does not bind to FHA2 (Liao *et al.*, 1999). These residues are well conserved in the FHA domains: Arg605 and Ser619 are absolutely conserved and the Arg617 and Arg620 are moderately conserved (Hofmann & Bucher, 1995). The phenyl ring of pTyr also contributes to binding because it is in close contact with the side-chains of Thr654, Asn655, and Arg617. Note that the pTyr aromatic group is in close contact with the Arg617 guanidino group, possibly by having an amino-aromatic interaction found in many protein structures (Burley & Petsko, 1986), except that the amino group does not lie exactly above the center of the phenyl ring. The binding is further strengthened by hydrophobic interactions between the Leu at the +2 position of the peptide and the side-chains of Ile681 and Asp683 from FHA2. The hydrophobicity at the +2 position seems to play an important role for the binding specificity, since ^{827}DIY(pY)LDI^{833}, another peptide derived from Rad9 which has an Asp at the +2 position, binds FHA2 with an order of magnitude lower affinity (Liao *et al.*, 1999). This preference for a hydrophobic residue at the +2 position is confirmed by combinatorial library screening (*vide infra*).

Comparison with other proteins that bind pTyr peptide

There are two other well-established pTyr peptide-binding domains: SH2 and PTB domains. Clearly, FHA2 has a very different structural topology and binding site from these two domains. However, we have tried to look for common features in pTyr peptide recognition. The pTyr peptide-binding mode of FHA2 is more similar to that of SH2 than that of PTB. This is consistent with the fact that the binding specificities of FHA2 and SH2 both depend on pTyr and the residues C-terminal to the pTyr, while PTB binds the pTyr peptides by recognizing the residues N-terminal to pTyr (reviewed by Kuriyan & Cowburn, 1997). Like FHA2, several conserved arginine, arginine/lysine, and serine residues of SH2 form ionic interactions with the phosphate group of pTyr (Figure 6). However, the phosphate-interacting residues of FHA2 reside in several loops and are solvent exposed, whereas in SH2 all except the serine residue are located on helices and β-sheets and the strictly conserved arginine residue (Arg154 in Src SH2) is buried. The buried Arg of SH2 is believed to be the critical residue that differentiates pTyr from pThr/pSer peptides. The guanidino group reaches the phosphate group of the pTyr peptide when the side-chain of this arginine residue exists in the extended conformation; no such interactions are possible for the much shorter pSer or pThr side-chains (Mayer *et al.*, 1992; Eck *et al.*, 1993; Kuriyan

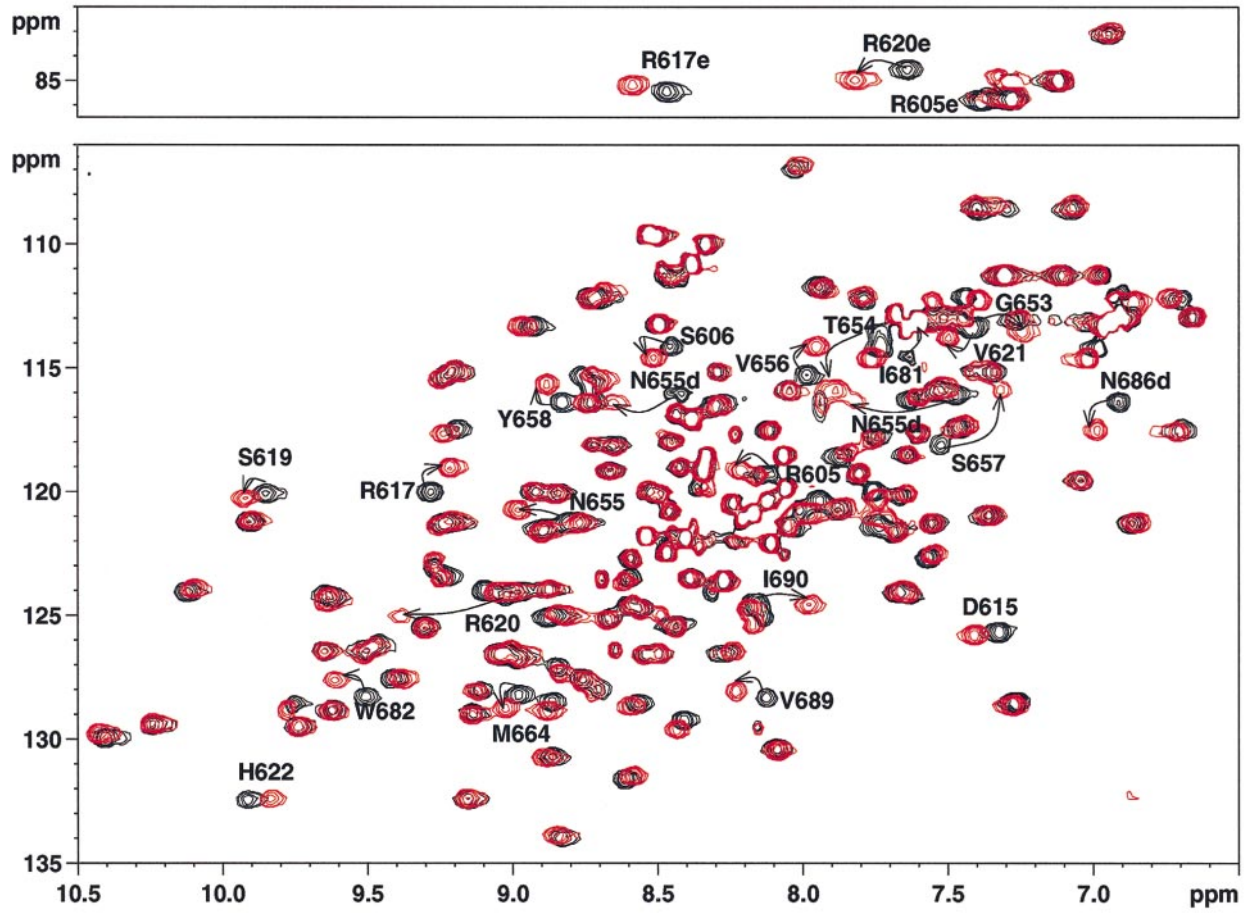

Figure 2. Superimposed ^{15}N-HSQC spectra of the free FHA2 (black) and FHA2 complexed with the pTyr peptide ^{826}EDI(pY)YLD^{832} derived from Rad9 (red). Only the peaks that undergo substantial shifts ($\geqslant$0.04 ppm for protons or $\geqslant$0.5 ppm for nitrogen atoms) are labeled with sequence numbers. The letters d and a stand for side-chain δ and ε positions, respectively. The Arg side-chain N$^{\varepsilon}$H peaks are shown at the top. The spectrum of free FHA2 was obtained using a 0.5 mM ^{15}N-labeled FHA2 sample; the spectrum of the complex was obtained by titrating with the peptide to ca. 1 mm concentration. The pH of the samples was maintained at pH 6.5 throughout the titration.

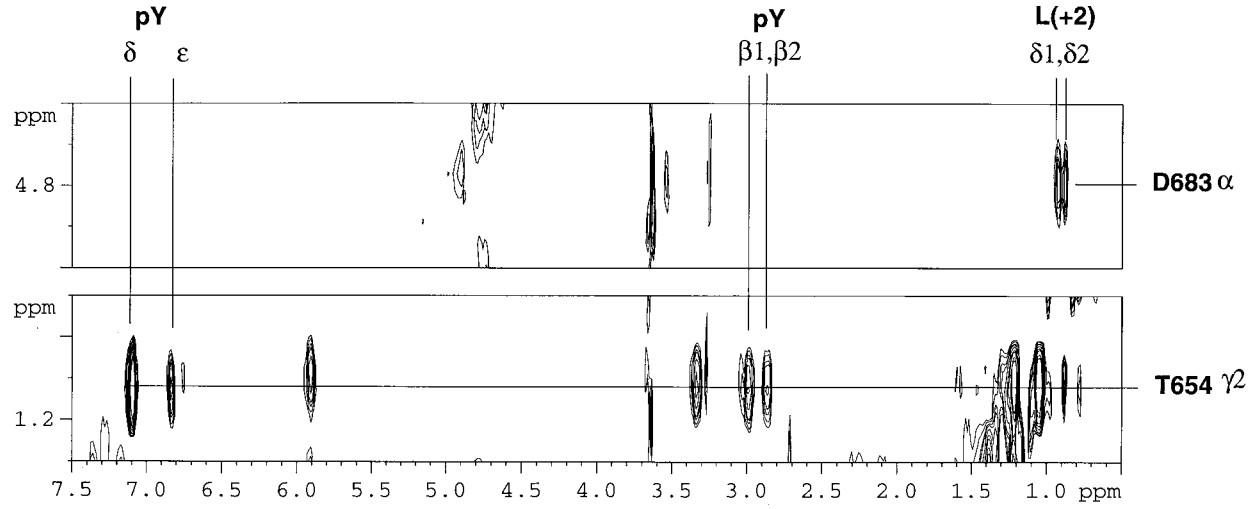

Figure 3. Selected regions of the 3D ^{13}C-filtered (f_2), ^{13}C/^{15}N-edited (f_3) NOESY spectrum of the FHA2 complexed with the Rad9 pTyr peptide. The intermolecular NOEs between Asp683 of FHA2 and the Leu (at the +2 position) of the peptide are shown at the top, and the NOEs between Thr654 of FHA2 and the pTyr of the peptide are shown at the bottom.

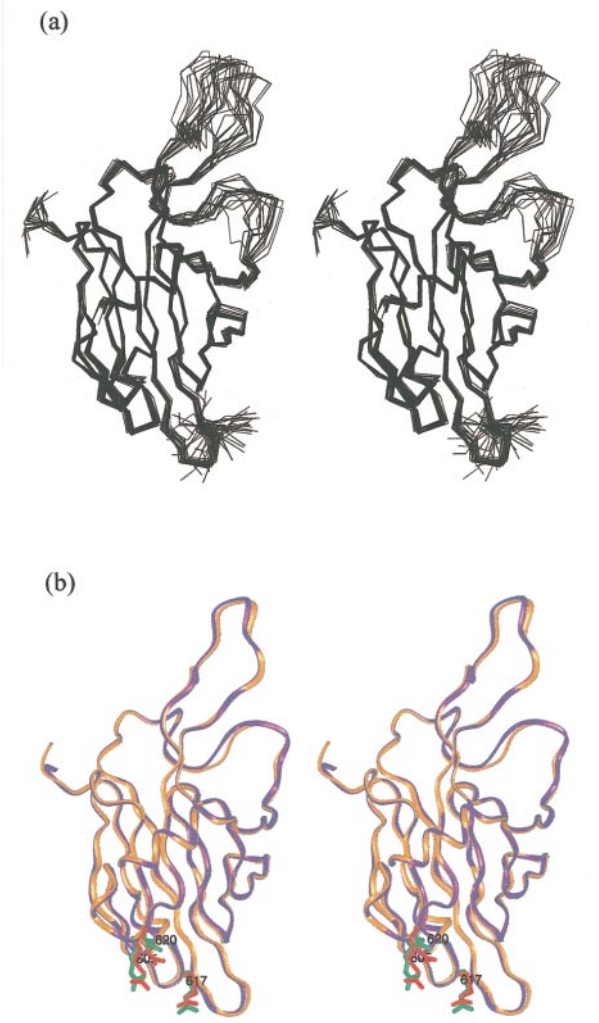

Figure 4. (a) Stereoview showing the superposition of the backbone C^{α} atoms of the 19 lowest-energy structures of FHA2 complexed with the pTyr peptide from Rad9. They were superimposed to best fit to the FHA2 domain (see Table 2 for details). (b) Stereoview of the superimposed ribbon diagram of the restrained minimized mean structures of free (orange) and complexed FHA2 (purple). The side-chains of the arginine residues that interact with the peptide phosphate group are also displayed, using green for the free state and red for the complexed state, respectively. The Figure was generated using Insight II (Molecular Simulations Inc.).

& Cowburn, 1997). The lack of such a residue in FHA2 could allow FHA2 to have less stringent phospho amino acid specificity than SH2. In both complexes, the peptides adopt extended conformations, but the SH2-bound peptide lies across the protein surface orthogonal to the central β-sheet while the FHA2-bound peptide lies near the ends of the β-sheets interacting with mostly loop residues. In SH2, the residues at the +1 (preferably polar ones for group ISH2 domains but hydrophobic ones for group IIISH2 domains) and +3 positions (preferably hydrophobic ones) of the peptide are important for binding specificity (Kuriyan & Cowburn, 1997) while in FHA2, the +2 residue is likely the one that directs the sequence specificity.

Design, synthesis, and screening of a pTyr peptide library

Although we have shown that the pTyr829 peptide of Rad9 binds to FHA2 in a specific fashion, the binding affinity is weak, raising the question of whether the pTyr peptide binding by FHA2 is physiologically relevant. To determine whether the FHA2 domain is capable of high-affinity binding to pTyr peptides, we have constructed a pTyr peptide library on TentaGel S resin, in which two residues immediately N-terminal and three residues C-terminal to the pTyr residue were randomized. Each of the random positions had an equal representation by 18 natural amino acids (except for cysteine and methionine) plus norleucine (Nle), which was used as a substitute of methionine. Therefore, the theoretical diversity of the library is 19^5 or 2.48×10^6. This library contains all of the possible hexapeptides and each bead carries ~100 pmol of a unique peptide sequence. A peptide linker, IBBRM (B = β-alanine), was synthesized to the C terminus of the random region (Yu & Chu, 1997), whereas glutamate and aspartate were added to the N terminus of the random region to improve aqueous solubility. Therefore, each member of the library bears the sequence: acetyl-EDXX(pY)XXXIBBRM-resin (X = random amino acid). In addition to a full-length peptide, each bead also carries a family of truncated peptides derived from the full-length peptide on that bead, which form a peptide ladder in a mass spectroscopy (MS) spectrum to allow for sequence identification of the full-length peptide *via* peptide ladder sequencing (Youngquist *et al.*, 1995; Hu *et al.*, 1999).

A total of 900 mg of the peptide library, which contained 2.57×10^6 beads, was screened against GST-FHA2 in three batches. Statistically, each possible pTyr hexapeptide is represented once in the library. Approximately 150 positive beads (identified by their turquoise color) were selected from this library, whereas control screening in the absence of GST-FHA2 always resulted in completely colorless beads. Out of the 150 beads, 53 produced high-quality MS spectra and their sequences were unambiguously determined (Table 3). A total of 25 beads gave only partial sequences C-terminal to the pTyr, with their N-terminal sequences unassigned. The rest of the beads gave poor mass spectra that could not be reliably analyzed. Analysis of the selected sequences revealed that FHA2 clearly binds to pTyr peptides of correct sequence contexts (Figure 7). FHA2 is most selective at the +2 position, where Tyr is by far the most preferred residue, followed by the structurally related Phe and, to a lesser extent, Leu and Met

Table 2. Structural statistics for the FHA2/Rad9 pTyr peptide complex structures

	⟨SA⟩	($\overline{SA}$)r
r.m.s.d. from experimental distance restraints (Å)[a]		
All (3158)	0.033 ± 0.001	0.032
FHA2: Sequential ($\|i-j\|=1$) (615)	0.040 ± 0.001	0.039
Medium ($1<\|i-j\|<5$) (307)	0.047 ± 0.002	0.045
Long range ($\|i-j\|\geqslant 5$) (1161)	0.029 ± 0.001	0.029
Intraresidue (898)	0.030 ± 0.002	0.030
Hydrogen bonds (80)	0.018 ± 0.003	0.016
Peptide:		
Sequential ($\|i-j\|=1$) (25)	0.000 ± 0.000	0.000
Medium ($\|i-j\|=2$) (5)	0.000 ± 0.001	0.000
Intraresidue (46)	0.001 ± 0.001	0.001
FHA2-peptide (21)[b]	0.008 ± 0.003	0.008
r.m.s.d. from backbone torsion angle restraints (°) (188)[c]	2.002 ± 0.049	2.067
r.m.s.d. from idealized covalent geometry:		
Bonds (Å)	0.003 ± 0.000	0.003
Angles (°)	0.465 ± 0.005	0.466
Impropers (°)	0.396 ± 0.011	0.401
Final energy:		
E_{L-J} (kcal/mol)[d]	−329 ± 69	−344
PROCHECK (Ramachandran plot)[e]		
Most favored regions (%)	84.5 ± 1.1	85.5
Additionally allowed region (%)	13.6 ± 1.1	12.9
Generously allowed region (%)	0.3 ± 0.4	0.0
Disallowed region (%)	1.6 ± 0.0	1.6
Atomic r.m.s.d. between ⟨SA⟩ and $\overline{SA}$ (Å):	Backbone	All heavy atoms
FHA2 residues 575-631, 643-705, and 714-729	0.36 ± 0.05	0.80 ± 0.05
Peptide residues 0 to +2	1.32 ± 0.40	2.18 ± 0.56
Atomic r.m.s.d. between free and complexed ($\overline{SA}$)r (Å):		
FHA2 residues 575-631, 643-705, and 714-729	0.43	0.93

⟨SA⟩ are the final 19 simulated annealing structures; $\overline{SA}$ is the mean structure obtained by averaging the coordinates of the individual SA structures best fit to each other (excluding the flexible N-terminal (573-574), loop (632-642 and 706-713), and C-terminal (730) residues, and the peptide residues); and ($\overline{SA}$)r is the restrained minimized mean structure obtained by restrained minimization of the mean structure $\overline{SA}$. The number of restraints is given in parentheses.

[a] None of the ⟨SA⟩ structures exhibited distance violations greater than 0.5 Å.

[b] Including three artificial distance restraints.

[c] The torsion angle restraints were derived by using TALOS (Cornilescu *et al.*, 1999).

[d] E_{L-J} is the Lennard-Jones van der Waals energy calculated with the X-PLOR PARMALLH6 protein parameters (Brünger, 1992) and is not included in the target function for simulated annealing or restrained minimization.

[e] The flexible loop (632-642 and 706-713) residues are excluded from the statistics.

(Nle). Clearly, a large hydrophobic side-chain is required for binding at this position, which is consistent with our structural study. Strong selectivity is also evident at the +1 and +3 positions, where large hydrophobic residues are again preferred (Figure 7). At the +1 position, Leu, Nle, and Phe are almost equally represented among the selected sequences, whereas Ile, Val, and Tyr are significantly less frequent. A similar pattern was observed at the +3 position, where Phe, Leu, and Nle are about equally preferred. There is also some selectivity for hydrophobic residues (e.g. Phe, Val, and Leu) at the −1 position, but this selectivity is much weaker than that of C-terminal residues. Very little, if any, selectivity was observed at the −2 position. In summary, the sequence specificity of the FHA2 domain resembles that of SH2 domains in the overall preference for large hydrophobic residues at three residues immediately C-terminal to pTyr. Residues beyond the −2 and +3 positions may also contribute to the overall binding affinity but were not examined here.

Characterization of binding of selected peptides by fluorescence resonance energy transfer

Three of the peptides in Table 3, each representing a different subfamily, were selected for further analysis. Peptide GF(pY)LYFIR (entry no. 3) features the most preferred amino acid residues at all positions that are important for binding. In peptide DV(pY)FYMIR (entry no. 28), Phe and Met at the +1 and +3 positions, respectively, are not the most preferred residues. Peptide IQ(pY)IYHIR (entry no. 14) has still less preferred residues at the +1 (Ile) and +3 (His) positions. These three peptides were individually synthesized on large scales with a dansyl group fused to their N termini, and tested for binding to FHA2 using fluorescence energy transfer (FRET) from protein tryptophan residues to the dansyl group. Binding assays were performed at a fixed concentration of the pTyr peptides and varying concentrations of the GST-FHA2 protein (Figure 8). Association was monitored by measuring the fluorescence yield of the dansyl group at 520 nm while exciting the tryptophan

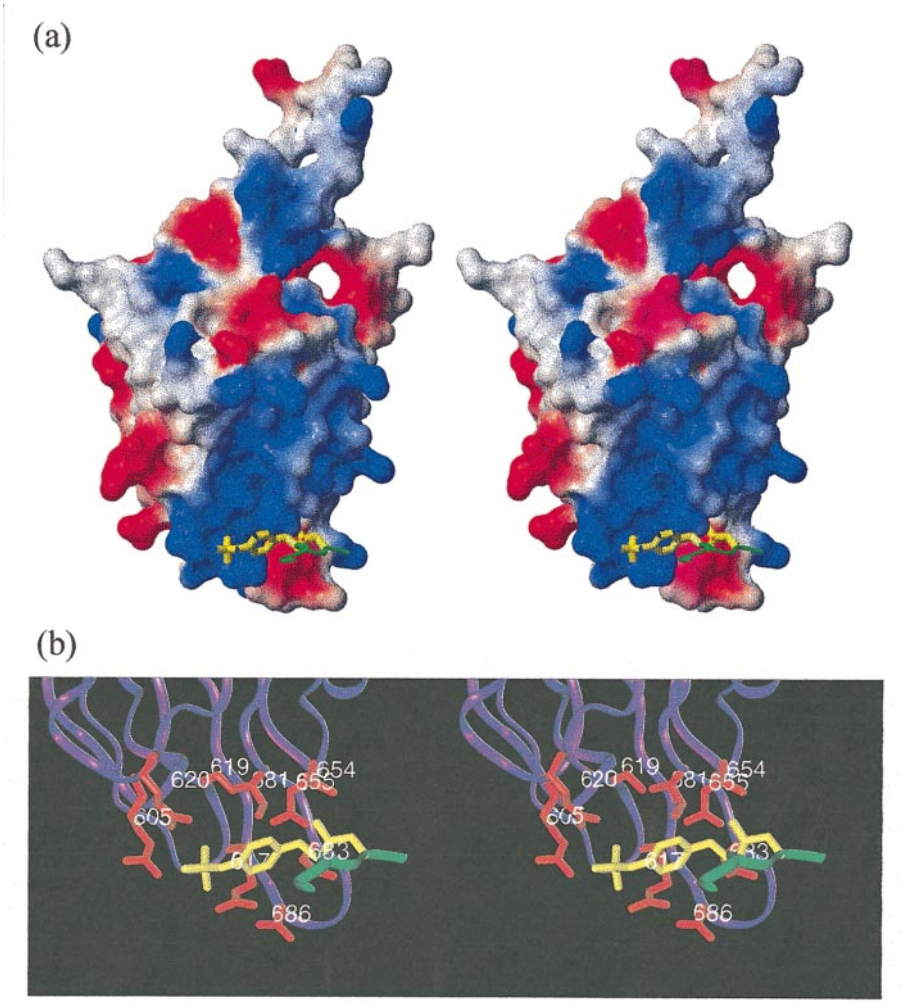

Figure 5. The binding interface for FHA2 and the Rad9 pTyr peptide (a) Surface representation of the FHA2 domain in complex with the peptide; (b) side-chain interactions of the peptide with the FHA2 domain. The backbone ribbons of FHA2 and the peptide are shown in purple and green, respectively. The side-chains of FHA2 and the peptide are shown in red and yellow, respectively. MOLMOL (Koradi *et al.*, 1996) and Insight II (Molecular Simulations Inc.) were used for (a) and (b), respectively.

residues at 290 nm. Peptide GF(pY)LYFIR (no. 3) showed the highest affinity to GST-FHA2, with a K_d of 1.1 μM. Peptide DV(pY)FYMIR bound GST-FHA2 less tightly, with a K_d of 5.0 μM. The third peptide, IQ(pY)IYHIR, showed little fluorescence enhancement with up to 10 μM GST-FHA2 protein so that the K_d value could not be determined by the FRET method (Table 4) Our NMR titrations confirmed that this peptide binds to FHA2, but less tightly, with a K_d of 100 μM (see below). To ensure that the observed binding is to the FHA2 domain but not to the GST portion, control experiments were carried out with GST only; no significant fluorescence enhancement was observed under the same conditions (Figure 8). Furthermore, when the untagged FHA2 domain was tested for binding to peptide GF(pY)LYFIR, a K_d value of 2.7 μM was obtained (Figure 8). These results demonstrate that the selected pTyr peptides are indeed specific ligands for the FHA2 domain.

Agreement between the complex structure and the library screening

We next pursued the possibility of determining the structure of the complex between FHA2 and one of the high-affinity pTyr peptides identified from the combinatorial library. Unfortunately, neither the peptide GF(pY)LYFIR nor its derivatives, DGF(pY)LYFIR and DDGF(pY)LYFIR, were sufficiently soluble for NMR studies. Thus, we have utilized the weaker-binding but more soluble peptide, IQ(pY)IYHIR, for our studies. The addition of two charged residues to the N terminus rendered the resulting peptide (Ac-DEIQ(pY)lY-HIR) sufficiently soluble to conduct NMR studies to map out the binding site on FHA2. The NMR

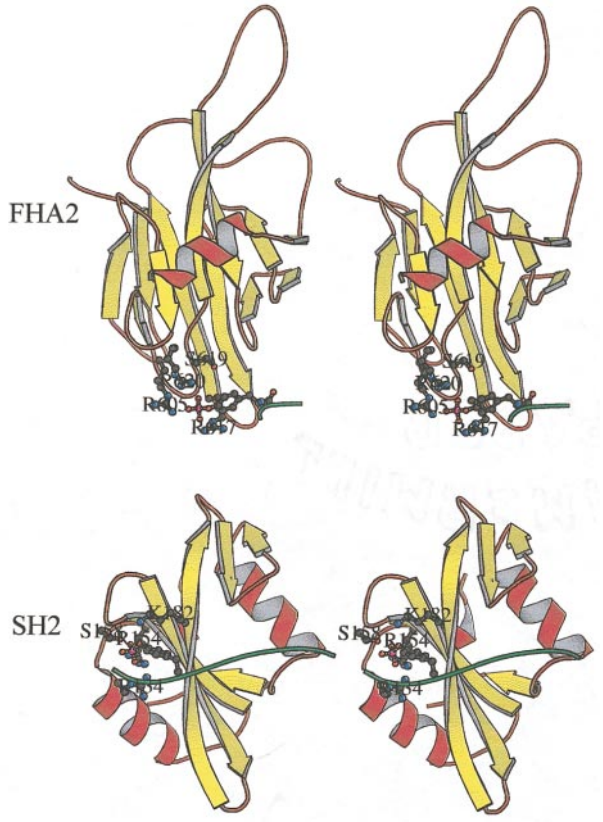

Figure 6. Schematic ribbon diagrams of the FHA2-Rad9 pTyr peptide and the SH2-pTyr peptide (Eck *et al.*, 1993) complex structures. The pTyr binding sites are also shown. The Figure was generated using MOLSCRIPT (Kraulis, 1991).

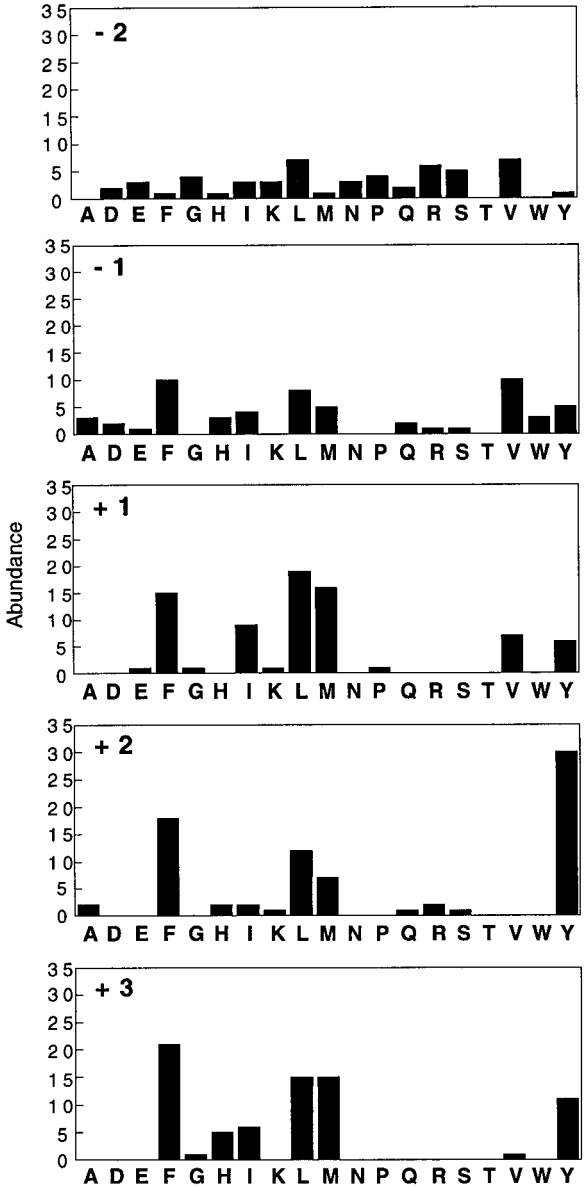

Figure 7. pTyr peptide sequence specificity for binding to the FHA2 domain. Displayed are the amino acid residues selected at the −2 to +3 positions relative to the pTyr residue. The *x* axis indicates the identity of the 19 amino acid residues in single letter codes, whereas abundance on the *y* axis represents the number of occurrence of an amino acid at a certain position (maximum 78). M, norleucine.

titration studies showed that the K_d value of this peptide is similar to that of the Rad9 pTyr peptide, and that similar residues were shifted in the ^{15}N-HSQC spectra. However, the magnitudes of shifts were smaller, and a smaller number of intermolecular NOEs were observed. Thus, complete determination of the complex structure was not performed. However, the results are sufficient to suggest that the two peptides interact with the same set of residues of FHA2.

Both NMR structure and library screening suggest that the residues C-terminal to the pTyr residue of the peptide are involved in the interaction with FHA2. In particular, the structure shows that a key interaction is mediated by the side-chains of the +2 residue and a hydrophobic surface on the FHA2 domain. Consistent with this mechanism, the result of library screening indicates that FHA2 shows the strongest selectivity at the +2 position.

Possible biological relevance of our results

Our results raise some interesting questions. First, why is the Rad9 pTyr829 sequence not selected from the library screening? Is Rad9 pTyr829 the physiological binding site of FHA2? The Rad9 sequence was not selected, most likely because it lacks a hydrophobic side-chain at the +3 position and therefore is weak binding. Among the 78 sequences in Table 3, none of them contained an Asp or Glu at the +3 position. Nevertheless, a number of the peptides selected from the library have very similar sequences to the Rad9 peptide

Table 3. Sequences of selected peptides from the library

Entry	Peptide sequence	Entry	Peptide sequence
1	RLpYLYF	40	RTpYFLF
2	MLpYLYF	41	SHpYFLF
3	GFpYLYF	42	PHpYMFF
4	XXpYLYF	43	LApYMFF
5	QVpYLYY	44	PDpYKFF
6	GFpYLYY	45	VLpYLFM
7	DYpYLYY	46	VFpYMFL
8	VYpYLFY	47	RVpYLFL
9	RQpYIYF	48	XXpYIFL
10	XXpYIYF	49	XXpYMFL
11	NLpYIYM	50	XXpYVFW
12	XVpYIYM	51	VFpYMLL
13	VVpYIYH	52	KYpYMMM
14	IQpYIYH	53	GLpYMML
15	RFpYIYL	54	LYpYLLM
16	XXpYLYM	55	LIpYLLM
17	KMpYLYL	56	LDpYVLM
18	EIpYLYI	57	RRpYMML
19	EVpYLYH	58	QFpYLLY
20	INpYVYH	59	PFpYMMF
21	PFpYVYH	60	XSpYMMF
22	VXpYVYL	61	XXpYMLF
23	IMPYVYM	62	XLpYMMY
24	YHpYMYL	6.3	EVpYYMF
25	XIPYMYM	64	SRpYYHY
26	NFpYFYL	65	NWpYFHY
27	XXpYFYL	66	XXpYFRY
28	DVpYFYM	67	XXpYYLF
29	LVpYFYM	68	XLpYMIF
30	VMPYYYM	69	XXpYLRF
31	KLpYEYY	70	LWpYLIY
32	HWpYFFL	71	LMpYFLL
33	FApYFFM	72	SFpYFLV
34	XMpYFFF	73	GYpYGAL
35	XXpYFFF	74	GVpYVSI
36	XIpYFFM	75	XXpYYKI
37	XXpYFFI	76	XXpYMLI
38	SVpYYFF	77	SApYIQG
39	XEpYYFL	78	XXpYPAI

M, norleucine; X, identity unknown.

(pYYLD): pYYLF (no. 67), pYFLF (no. 40 and 41), pYFLL (no. 71), and pYFLV (no. 72), where large hydrophobic or aromatic residues are selected for the three residues C-terminal to the pTyr. The second question is more difficult to answer, since the actual Rad53 binding site(s) of Rad9 is still unknown. However, among the 13 possible pTyr sites, pTyr829-containing peptide binds to FHA2 with the highest affinity and therefore is the most likely candidate (Liao *et al.*, 1999) if the biological binding site of FHA2 is a pTyr site. It is less likely that the residues outside the −3 to +3 region are involved in binding, since a Rad9 peptide extended to 13 residues (^{825}DEDI(pY)YLDIRIGD^{837}) did not

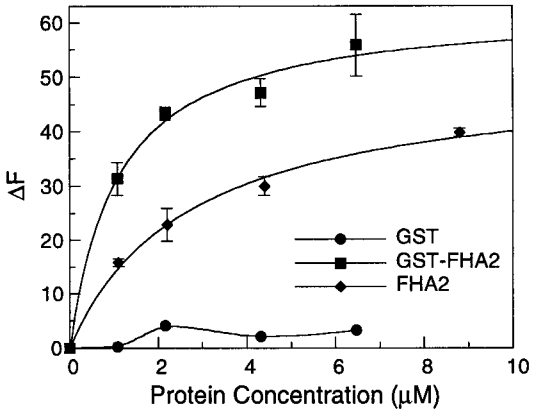

Figure 8. Binding assay of the peptide DNS-GF(pY)-LYFIR. The concentration of peptide for assay with GST-FHA2 and GST was 96 nM; for assay with FHA2 it was 432 nM.

Table 4. Dissociation constants of pTyr peptides to FHA2

Peptide	K_d (μM)	
	GST-FHA2	FHA2
GF(pY)LYFIR	1.1 ± 0.3	2.7 ± 0.6
DV(pY)FYMIR	5.0 ± 0.6	ND
IQ(pY)IYHIR	~100	ND

ND, not determined.

bind FHA2 any tighter than the shorter peptide (unpublished data). Rather, it may require other Rad9 segments, which are distal in primary sequences but spatially close to pTyr829, to complete the binding to FHA2 of Rad53. It is also possible that FHA2 binds to a pThr site of Rad9, since our preliminary data indicate that FHA2 also binds some pThr peptides (unpublished results).

FHA domains have dual phosphopeptide specificity

In our earlier paper (Liao *et al.*, 1999) we proposed that FHA domains could have pTyr and pSer/pThr dual specificity, or FHA domains from different proteins could have different specificity. Our preliminary results from screening pThr, pSer, and pTyr libraries against FHA1 and FHA2 domains suggest that both domains are capable of binding to all three types of phosphopeptides (unpublished results). Since the pSer/pThr specificity is widely accepted for FHA domains (Durocher *et al.*, 1999; Li *et al.*, 1999; Yaffe & Cantley, 1999), our demonstration of the pTyr specificity for the FHA2 domain here provides conclusive experimental evidence for our dual specificity proposal. Thus, FHA domains represent the first phosphoprotein-binding module that has pTyr and pSer/pThr dual specificity. The structural determination of an FHA-pThr peptide complex is being completed in our laboratory and will be reported shortly.

Materials and Methods

Materials

TentaGel S NH_2 resin, Wang resin, *N*-9-fluorenylmethoxycarbonyl (Fmoc)-amino acids, 1-hydroxybenzotriazole (HOBT) and 2-(1*H*-benzotriazole-l-yl)-1,1,3,3-tetramethyluronium hexafluorophosphate (HBTU) were purchased from Advanced ChemTech (Louisville, KY). *N*-Hydroxysuccinimidobiotin, acetylglycine, *N*-acetyl-D,L-alanine, 5-bromo-4-chloro-3-indolyl phosphate, streptavidin-alkaline phosphatase and dansyl chloride were obtained from the Sigma Chemical Co. (St. Louis, MO). All other chemicals were purchased from Aldrich Chemical (Milwaukee, WI).

The FHA2 domain of Rad53 (residues 573-730) were cloned into pGEX-4T vector (Pharmacia Biotech) for expression of glutathione *S*-transferase (GST) fusion proteins in BL21(DE3) (Novagen). The fusion proteins (GST-FHA2) were purified using glutathione agarose (Sigma). The GST tag was removed by thrombin (Sigma) digestion and gel-filtration chromatography. Isotope-labeled proteins were expressed in M9 media containing $^{15}NH_4Cl$ and [^{13}C]glucose correspondingly. The purified Rad9 pTyr peptide (EDI(pY)YLD) was purchased from Genemed Synthesis, Inc. (S. San Francisco, CA).

NMR experiments

NMR experiments were performed on a Bruker DMX-600 or DRX-800 spectrometer at 20 °C. The protein concentration was 0.5 mM. The samples contained 10 mM sodium phosphate, 1 mM DTT, and 1 mM EDTA in 95 % H_2O/5 % ^2H_2O or 100 % ^2H_2O at pH 6.5. Intermolecular (FHA2-Rad9 pTyr peptide) NOEs were identified from 3D ^{13}C-edited (f_2), $^{13}C/^{15}N$-filtered (f_3) NOESY (Lee *et al.*, 1994), and the intramolecular NOE assignments of the pTyr peptide were obtained using 2D $^{13}C/^{15}N$-filtered NOESY (Ikura & Bax, 1992; Lee *et al.*, 1994) using the complexed sample ([$^{13}C/^{15}N$-FHA2]:[pTyr peptide] ~ 1:2). The intramolecular NOEs for the FHA2 domain in the complexed form were identified using 3D ^{15}N-edited NOESY (Sklenar *et al.*, 1993; Grzesiek & Bax, 1993) and ^{13}C-edited NOESY (Fesik & Zuiderweg, 1988) using the complexed sample. A mixing time of 100 ms was used for all the NOESY data. The NOESY data were processed and analyzed using XWIN-NMR 2.6 (Bruker) or Felix 95.0 (Molecular Simulations Inc.). Structural calculations were conducted using a simulated annealing method (Nilges *et al.*, 1988) within X-PLOR (Brünger, 1992) using the distance restraint derived from the identified NOEs and H-bonds as well as the backbone torsion angle restraints derived from the TALOS program (Cornilescu *et al.*, 1999). For the complex structure calculation, three additional distance restraints (4.3(±0.3) Å for the C^ζ of Arg605, Arg617, and Arg620 to the P atom of pTyr) were included, since the NMR titration data (Figure 2) and the complex structural calculation without these three restraints (not shown) clearly indicated that these three Arg side-chains are involved in binding (approximately 4-5 Å from the Arg N^η atom to the phosphate group O atom). The structures were analyzed by X-PLOR (Brünger, 1992), PROCHECK (Laskowski *et al.*, 1993), and MOLMOL (Koradi *et al.*, 1996). For both the free and the pTyr peptide-complexed FHA2 structures, the final 19 structures with lowest energy were selected from a total of 60 calculated ones.

Peptide-binding experiments were performed by recording a series of 2D ^{15}N-HSQC spectra (Grzesiek & Bax, 1993) on uniformly ^{15}N-labeled protein samples with different concentrations of peptides. The pH of the samples was maintained at pH 6.5 throughout the titration.

Synthesis of the phosphotyrosyl peptide library

TentaGel S NH_2 resin (0.3 mmol/g loading, 2.86×10^6 beads/g, 80-100 μm) was used as the solid support for the peptide library. Synthesis was carried out on a 5.0 g scale on a home-made peptide synthesis apparatus using standard Fmoc/HBTU/HOBT chemistry (Bodanszky, 1993). A common linker of four amino acid residues. BBRM (B = β-alanine), was first synthesized on the resin by using a fourfold excess of amino acids (Yu & Chu, 1997). The five random positions were generated by using the split-synthesis method, resulting in a one-bead-one-peptide library (Lam *et al.*, 1991; Furka *et al.*, 1991). The coupling reaction at each random position was carried out twice with a fivefold excess of the proper amino acid for three hours to ensure complete coupling. To produce a small percentage of truncated peptides for later sequence analysis, 10 % (mol/mol) acetylglycine was added to the coupling reactions during the synthesis of the random residues and phosphotyrosine (for all amino acids except for norleucine, glutamine, and isoleucine; Youngquist *et al.*, 1995; Hu *et al.*, 1999). For norleucine and glutamine, 10 % acetylalanine was used, whereas a 1:1 mixture of acetylglycine and acetylalanine (total 10 %) was used during the coupling of isoleucine. After library synthesis was complete, deprotection was carried out using a cocktail containing 90 % (v/v) TFA,

2% anisole, 3% ethanedithiol, and 5% thioanisole for one hour at room temperature. The resin was washed with CH_2O_2 (10 × 10 ml) and methanol (5 × 10 ml), dried under vacuum, and stored at −20 °C.

Synthesis of dansylated peptides

Peptides were synthesized on Wang resin using standard Fmoc/HBTU/HOBT chemistry on a 0.15-mmol scale. Coupling reactions were carried out with a fourfold excess of amino acids for at least one hour and the completion of the reaction was ensured by ninhydrin tests. Addition of a dansyl group to the N-terminal amino group was effected by incubating the protected, resin-bound peptide with 1.5 equivalents of dansyl chloride and three equivalents of triethylamine for 45 minutes at room temperature. Deprotection of the side-chains and cleavage of the peptide off the resin were carried out using the same cocktail as described above. The resulting peptide solution was drained into a glass vial and the solvent was evaporated under a flow of nitrogen gas. The semi-solid residue was triturated with anhydrous diethyl ether (3 × 10 ml) and stored at −20 °C. The crude product was purified by reversed-phase HPLC before use. The identity of all dansylated peptides was confirmed by matrix-assisted laser desorption ionization mass spectrometry (MALDI MS) analysis.

Preparation of biotinylated GST-FHA2

Biotinylated GST-FHA2 was obtained by treating GST-FHA2 (114 μM) with 2.5 molar equivalents of N-hydroxysuccinimidobiotin (NHS-biotin) in PBS buffer (50 mM Na/PO_4, 350 mM NaCl (pH 7.4)) for three hours before the reaction was quenched by the addition of 4 μl of 2-aminoethanol (17 M). The biotinylated protein was quickly frozen and stored at −80 °C until use.

On-bead screening of the pTyr peptide library against GST-FHA2

Library screening was conducted in three separate batches. For each batch, 300 mg of resin was incubated with DMF (2 × 10 ml) for 30 minutes and exhaustively washed with water (20 × 10 ml) in a plastic column fitted with a filter/disc (Bio-Rad) before use. After incubation of the resin in 3.5 ml of TBS buffer (25 mM Tris-HCl (pH 7.4), 150 mM NaCl, 1 mg/ml gelatin) for one hour, 70 μl of biotinylated GST-FHA2 (final concentration = 0.9 μM) was added to the solution. After overnight incubation at room temperature, the solution was drained, and 2.5 ml of TBS buffer, 70 μl of 1.5 M potassium phosphate (pH 7.4), and 10 μl of streptavidin-alkaline phosphatase (final concentration = 22 nM) were added to the resin. After incubation at room temperature for 15 minutes, the solution was again drained and the resin was washed with PBS buffer (10 ml) and then TBS buffer (10 ml). The resin was resuspended in 12 ml of TBS buffer (25 mM Tris (pH 8.5), 150 mM NaCl) in a Petri dish, and 6 mg of 5-bromo-4-chloro-3-indolyl phosphate was added to the mixture. The Petri dish was placed on a shaker at room temperature. Positive beads stained with intense turquoise color emerged from the dish within one hour. The staining reaction was stopped by treating the resin with 4 ml of 6 M guanidine-HCl for 20 minutes. The resin was washed with double-distilled water (10 × 3 ml) and the positive beads were removed from the dish and placed in individual Eppendorf tubes using a pipette under a low-power microscope. A control screening was conducted under the same conditions except that no GST-FHA2 protein was included in the screening. No colored beads were observed.

Peptide sequencing by MALDI mass spectrometry

Each positive bead selected from the library was treated with 20 μl of a CNBr solution (20 mg/ml in 70% formic acid) in a microcentrifuge tube in the dark for 20-24 hours at room temperature. After evaporation of the solvent under vacuum, the residue was dissolved in 5 μl of 0.1% TFA solution. For MALDI MS analysis, 1 μl of the peptide solution was mixed with 2 μl of a saturated solution of α-cyano-4-hydroxycinnamic acid in 50% aqueous acetonitrile. A 1 μl volume of the mixture was spotted onto the MALDI sample slide. After crystallization of the mixture, the sample was analyzed on a Kratos Kompact MALDI-III mass spectrometer.

Determination of binding constants

Binding of the dansylated peptides to GST-FHA2 or free FHA2 domain was monitored by fluorescence energy transfer from tryptophan residues in the protein to the dansyl group in the peptides on a Perkin-Elmer LS-5 spectrofluorimeter. The tryptophan residues were excited at 290 nm while the emission of the dansyl group at 520 nm was monitored. All binding assays were carried out in a phosphate buffer (4.3 mM Na/PO_4, 1.5 mM K/PO_4, 140 mM NaCl, 2.7 mM KCl (pH 7.3)). Typically, the mixture of the peptide (0.2 μM) and varying concentrations of the protein (1-10 μM) was incubated for 10-20 minutes before the reading was taken. The net fluorescence increase (ΔF) at 520 nm due to energy transfer was obtained for each protein concentration by subtracting the background fluorescence caused by the peptide, the protein, and the buffer solution from the total fluorescence. The experimental data were fitted against the equation:

$$\Delta F = \Delta F_{max} \cdot C/(K_d + C)$$

where K_d is the dissociation constant, ΔF is the fluorescence enhancement at a given protein concentration C, and ΔF_{max} is the maximum fluorescence enhancement. Protein concentrations were determined by Bradford assay. The dansylated peptides were dissolved in 50% DMF and their concentrations were determined by measuring the absorbance of the dansyl group at 350 nm ($\varepsilon_{350} = 4.57 \times 10^3\ M^{-1}\ cm^{-1}$).

Accession numbers

Coordinates for the refined FHA2 and its complex structure with the Rad9 pTyr peptide have been deposited in the RCSB PDB (accession numbers are 1FHQ and 1FHR, respectively) and will be released upon publication of this work.

Acknowledgments

The authors thank Dr Frits Abildgaard at NMRFAM for the filtered 2D and 3D NOESY pulse sequences,

Mei-I Su for the help with protein purification, the Ohio Supercomputer Center for the T94 Cray supercomputer resource grant, the Ohio Board of Regents for funding of the 800 MHz NMR, and NIH for financial support (CA69472).

References

Allen, J., Zhou, Z., Siede, W., Friedberg, E. & Elledge, S. (1994). The SAD1/RAD53 protein kinase controls multiple checkpoints and DNA damage-induced transcription in yeast. *Genes Dev.* **8**, 2401-2415.

Bodanszky, M. (1993). *Principles of Peptide Synthesis*, 2nd edit., Springer-Verlag, New York.

Boudrez, A., Beullens, M., Groenen, P., Van Eynde, A., Vulsteke, V., Jagiello, I., Murray, M., Krainer, A. R., Stalmans, W. & Bollen, M. (2000). NIPPI-mediated interaction of protein phosphatase-1 with CDC5L, a regulator of pre-mRNA splicing and mitotic entry. *J. Biol. Chem.* In the press.

Brown, A., Lee, C., Schwarz, J., Mitiku, N., H., P.-W. & Chung, J. (1999). A human Cds1-related kinase that functions downstream of ATM protein in the cellular response to DNA damage. *Proc. Natl Acad. Sci. USA,* **96**, 3745-3750.

Brünger, A. T. (1992). X-PLOR. *A System for X-ray Crystallography and NMR*, Yale University, New Haven, Connecticut.

Burley, S. K. & Petsko, G. A. (1986). Amino-aromatic interactions in proteins. *FEBS Letters,* **203**, 139-143.

Cornilescu, G., Delaglio, F. & Bax, A. (1999). Protein backbone angle restraints from searching a database for chemical shift and sequence homology. *J. Biomol. NMR,* **13**, 289-302.

Durocher, D., Henckel, J., Fersht, A. R. & Jackson, S. P. (1999). The FHA domain is a modular phosphopeptide recognition motif. *Mol. Cell,* **4**, 387-394.

Eck, M., Shoelson, S. & Harrison, S. (1993). Recognition of a high-affinity phosphotyrosyl peptide by the Src homology-2 domain of p561ck. *Nature,* **362**, 87-91.

Fesik, A. W. & Zuiderweg, E. R. P. (1988). Heteronuclear three-dimensional NMR spectroscopy. A strategy for the simplification of homonuclear two-dimensional NMR spectra. *J. Magn. Reson.* **78**, 588-593.

Furka, A., Sebestyen, F. & Asgedom, M. & Dibo, G. (1991). General method for rapid synthesis of multicomponent peptide. *Int. J. Pept. Protein Res.* **37**, 487-493.

Grzesiek, S. & Bax, A. (1993). The importance of not saturating H_2O in protein NMR. Application to sensitivity enhancement and NOE measurements. *J. Am. Chem. Soc.* **115**, 12593-12594.

Hammet, A., Pike, B. L., Mitchelhill, K. I., Teh, T., Kobe, B., House, C. M., Kemp, B. E. & Heierhorst, J. (2000). FHA domain boundaries of the dun1p and rad53p cell cycle checkpoint kinases. *FEBS Letters,* **471**, 141-146.

Hofmann, K. & Bucher, P. (1995). The FHA domain: a putative nuclear signaling domain found in protein kinases and transcription factors. *Trends Biochem. Sci.* **20**, 347-349.

Hu, Y. J., Wei, Y., Zhou, Y., Rajagopalan, P. T. R. & Pei, D. (1999). Determination of substrate specificity for peptide deformylase through the screening of a combinatorial peptide library. *Biochemistry,* **38**, 643-650.

Ikura, M. & Bax, A. (1992). Isotope-filtered 2D NMR of a protein peptide complex - study of a skeletal-muscle myosin light chain kinase fragment bound to calmodulin. *J. Am. Chem. Soc.* **114**, 2433-2440.

Koradi, R., Billeter, M. & Wuthrich, K. (1996). MOLMOL: a program for display and analysis of macromolecular structures. *J. Mol. Graphics,* **14**, 51-55.

Kraulis, P. J. (1991). MOLSCRIPT: a program to produce both detailed and schematic plots of protein structures. *J. Appl. Crystallog.* **24**, 946-950.

Kuriyan, J. & Cowburn, D. (1997). Modular peptide recognition domains in eukaryotic signaling. *Annu. Rev. Biophys. Biomol. Struct.* **26**, 259-288.

Lam, K. S., Salmon, S. E., Hersh, E. M., Hruby, V. J., Kazmierski, W. M. & Knapp, R. J. (1991). A new type of synthetic peptide library for identifying ligand-binding activity. *Nature,* **354**, 82-84.

Laskowski, R. A., MacArthur, M. W., Moss, D. S. & Thornton, J. M. (1993). PROCHECK: a program to check the stereochemical quality of protein structures. *J. Appl. Crystallog,* **26**, 283-291.

Lee, W., Revington, M. J., Arrowsmith, C. & Kay, L. E. (1994). A pulsed-field gradient isotope-filtered 3D C-13 HMQC-NOESY experiment for extracting intermolecular NOE contacts in molecular-complexes. *FEBS Letters,* **350**, 87-90.

Li, J., Smith, G. P. & Walker, J. C. (1999). Kinase interaction domain of kinase-associated protein phosphatase, a phosphoprotein-binding domain. *Proc. Natl Acad. Sci. USA,* **96**, 7821-7826.

Liao, H., Byeon, I. J. & Tsai, M. D. (1999). Structure and function of a new phosphopeptide-binding domain containing the FHA2 of Rad53. *J. Mol. Biol.* **294**, 1041-1049.

Matsuoka, S., Huang, M. & Elledge, S. (1998). Linkage of ATM to cell cycle regulation by the Chk2 protein kinase. *Science,* **282**, 1893-1897.

Mayer, B. J., Jackson, P. K., Van Etten, R. A. & Baltimore, D. (1992). Point mutations on the abl SH2 domain coordinately impair phosphotyrosine binding *in vitro* and transforming ability *in vivo*. *Mol. Cell. Biol.* **12**, 609-618.

Nilges, M., Clore, G. & Gronenborn, A. (1988). Determination of three-dimensional structures of proteins from interproton distance data by dynamical simulated annealing from a random array of atoms. Circumventing problems associated with folding. *FEBS Letters,* **239**, 129-136.

Oishi, I., Sugiyama, S., Otani, H., Yamamura, H., Nishida, Y. & Minami, Y. (1998). A novel *Drosophila* nuclear protein serine/threonine kinase expressed in the germline during its establishment. *Mech. Dev.* **71**, 49-63.

Pawson, T. & Scott, J. (1997). Signaling through scaffold, anchoring, and adaptor proteins. *Science,* **278**, 2075-2080.

Sklenar, V., Piotto, M., Leppik, R. & Saudek, V. (1993). Gradient-tailored water suppression for ^{1}H-^{15}N HSQC experiments optimized to retain full sensitivity. *J. Magn. Reson. ser. A,* **102**, 241-245.

Sun, Z., Hsiao, J., Fay, D. & Stern, D. (1998). Rad53 FHA domain associated with phosphorylated Rad9 in the DNA damage checkpoint (see comments). *Science,* **281**, 272-274.

Yaffe, M. B. & Cantley, L. (1999). Grabbing phosproteins. *Nature,* **402**, 30-31.

Youngquist, R. S., Fuentes, G. R., Lacey, M. P. & Keough, T. (1995). Generation and screening of combinatorial peptide libraries designed for rapid

sequencing by mass-spectrometry. *J. Am. Chem. Soc.* **117**, 3900-3906.

Yu, Z. & Chu, Y.-H. (1997). Combinatorial epitope search: pitfalls of library design. *Bioorg. Med. Chem. Letters*, **7**, 95-98.

Zheng, P., Fay, D., Burton, J., Xiao, H., Pinkham, J. & Stern, D. (1993). SPK1 is an essential S-phase-specific gene of *Saccharomyces cerevisiae* that encodes a nuclear serine/threonine/tyrosine kinase. *Mol. Cell. Biol.* **13**, 5829-5842.

Edited by P. Wright

(Received 5 July 2000; received in revised form 3 August 2000; accepted 4 August 2000)